MECHANICAL ANALYSIS AND NUMERICAL CALCULATION OF BONDING STRENGTH MEASUREMENT BY INTERFACIAL INDENTATION METHOD①

Yi Maozhong[1], Huang Baiyun[1], Dai Yao[2], He Jiawen[3] and Zhou Huijiu[3]
1 State Key Laboratory for Powder Metallurgy, Central South University of Technology, Changsha 410083, P. R. China
2 Institute of Armoured Force Engineering, Beijing 100072, P. R. China
3 State Key Laboratory for Mechanical Behavior of Metallic Materials, Xi' an Jiaotong University, Xi' an 710049, P. R. China

ABSTRACT Interfacial indentation is a new method for the evaluation of the bonding strength of the thick coating with good adhesion to the substrate. Based on the conservation of energy and Griffith principle, the formula of the bonding stress is obtained. The approximate stress value is gotten using numerically calculated and experimental results. Semi-analytic method of lines(MOL) and method of arbitrary lines(MAL) are used in the numerical calculation. Compared with finite element method(FEM), the efficiency and precision of the calculation is higher.

Key words coating interfacial indentation bonding strength mechanical analysis numerical calculation

1 INTRODUCTION

The bonding strength between coating and substrate is the most important property evaluating the quality of the coating and also a basis controlling and improving coating technology. So far, it is a non-standardized, unperfect and popular question[1] which user and researcher pay close attention to. Moreover, with the development of vaccum plasma spray and high velocity oxy-fuel spray techniques, the strength is improved greatly. Because of the restriction of the cohesion strength of cement used in the traditional pull-off test, the test is not suitable for evaluating the strength of the thick coating with good adhesion to the substrate[2]. A new interface indentation test shown in Fig. 1 is a suitable and promising method[3], but the Vicker hardness tester, on which the grading loading is performed, is used in the test, the length of the interface crack or the parameters in connection with the crack indicate the strength[3].

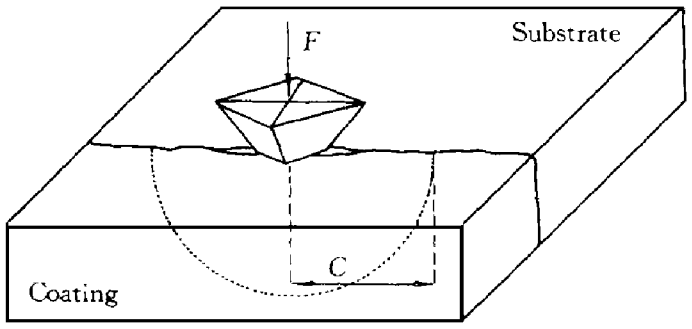

Fig. 1 Principle of interfacial indentatian test

The curve of load-indentation depth and the critical load (F_w) corresponding to the interface cracking can be measured at one tested point by a new indentation tester with continuous loading and unloading, and with the monitoring system for acoustic emission signal. The tester makes the test simpler and faster[5]. The paper deals

① Project 59471065 supported by the National Natural Science Foundation of China
Received Aug. 15, 1997; accepted Nov. 27, 1997

with the mechanical analysis of the interface indentation test and the numerical calculation by method of lines and method of arbitrary lines. The bonding strength value can be obtained by the calculated and experimental result.

2 MECHANICAL ANALYSIS OF INTERFACE INDENTATION TEST

Although there is a good relationship[5] between the bonding strength and the critical load (F_w) measured by the interface indentaion test, it is very difficult to set up the mechanical model to describe quantitatively the relationship. The reasons are that (1) geometrically, there is a huge difference of order of magnitude between the thickness of the coating and the one of the substrate; (2) physically, the mechanical behaviour of the coating is different from that of the substrate; (3) mathematically, the deformation and force near the interface possess high gradient; (4) the test is two phase and three dimension question. The reasons make it impossible to obtain the closed analytic solution to the question of the complicated test[6]. Therefore, the method combining the numerical calculation with the experimental measurement is used, the conservation of energy is a basis of analysing the question in the paper.

The expression of the total work for the creation of the indentation, W_t, is

$$W_t = U_e + U_p + \Gamma + W_f \tag{1}$$

where U_e is an elastic deformation energy of tested specimen, U_p is a plastic deformation energy, Γ is an interface energy, W_f is an frictional work between the indenter and the specimen. Because Vicker indenter is an obtuse angle, W_f may be neglected, and Eq. (1) is

$$W_t = U_e + U_p + \Gamma \tag{2}$$

where W_t is equal to the area of OAC in Fig. 2, Point A is the load value and corresponding to indentation depth C without interface crack. Theoretically, the load value CA line can be gotten by numerical calculation. Point B is the experimental value corresponding to interface cracking. So, area OAB is the strain energy (ΔU) released by the interface cracking. The average bonding energy can be expressed as

$$\gamma = -\Delta U / \Delta A \tag{3}$$

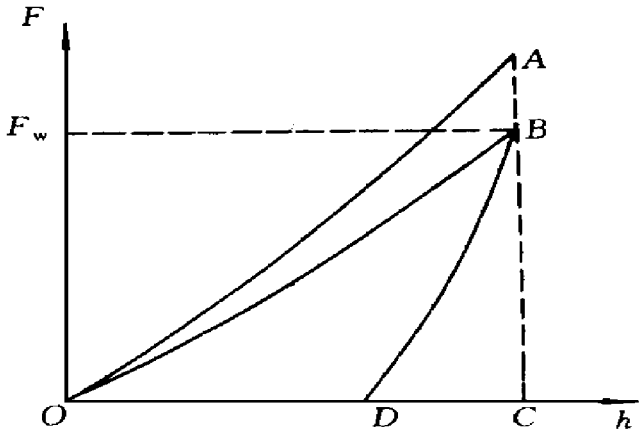

Fig. 2 Schematic load F vs. indentation depth h under elastic-plastic state

where ΔA is the area of the interface crack extension. According to Griffith Criterion the energy difference can be expressed as

$$\Delta\Gamma = -\Delta U = \iint_A \frac{1}{2}\tilde{\sigma}_{i2}(x_1, 0, x_3) \cdot n_2 \tilde{u}_i(x_1, 0, x_3)\, dA \tag{4}$$

where $\tilde{\sigma}_{i2}(x_1, 0, x_3)$ is the interface bonding stress, $\tilde{u}_i(x_1, 0, x_3)$ is the opening displacement value of the interface, that is

$$\tilde{u}_i(x_1, 0, x_3) = \tilde{u}_i^+(x_1, 0_+, x_3) - \tilde{u}_i^-(x_1, 0_-, x_3) \tag{5}$$

because the mechanical properties of the coating are different from that of the substrate, and the geometrical shape of the specimen is unsymmetrical, in Eq. (4), we have

$$\tilde{\sigma}_{12} \neq 0, \quad \tilde{\sigma}_{32} \neq 0 \tag{6}$$

that is, there exist shear stresses. But, the work done by the shear stresses is much smaller than the interface energy, and can be neglected for approximation. Eq. (4) can be

$$\Delta\Gamma = \frac{1}{2}\iint_A \tilde{\sigma}_{22}(x_1, 0, x_3) \cdot \tilde{u}_2(x_1, 0, x_3)\, dA \tag{7}$$

Suppose that the interface bonding stress is a constant under a certain technology and measuring condition. Eq. (7) can be expressed as

$$\Delta\Gamma = \frac{1}{2}\tilde{\sigma}_{22}\iint_A \tilde{u}_2(x_1, 0, x_3)\,dA \qquad (8)$$

The opening displacement field of the interface can be calculated by the numerical method, $\Delta\Gamma$ can be obtained by the calculated and experimental results. So, according to Eq. (8), the bonding strength value σ_{22} can be gotten.

According to above mentioned elastic-plastic state analysis, under linear elastic state, we have

$$W_t = U_e + \Gamma \qquad (9)$$

it is similar to Eq(8).

3 CALCULATION MODEL

Because the geometric shape of specimen, loading zone and restraining conditions in Fig. 1 are symmetric, we analyse and calculate only the half of the bulk specimen. The model of the calculation is shown in Fig. 3.

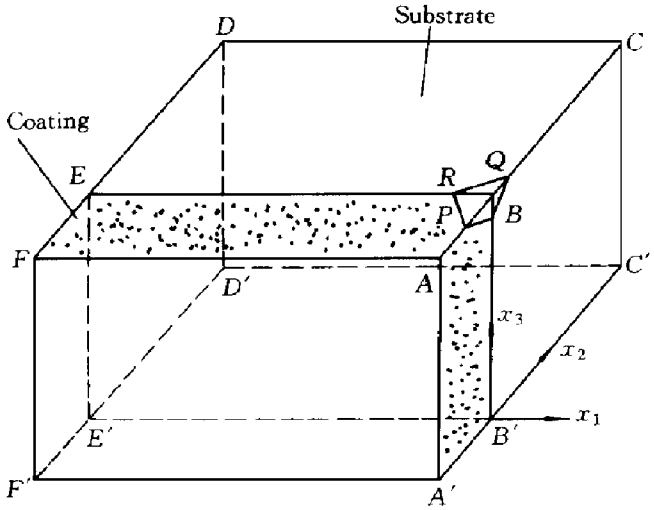

Fig. 3 Model of calculation

Boundary condition:

(1) Bottom face $ABCDEF$: $u_y = 0$, $u'_{zx} = 0$, $\tau_{zx} = 0$;

(2) Symmetric face $ABCCBA$: $u_x = 0$, $\tau_{xy} = 0$; $\tau_{xx} = 0$;

(3) Top face $ABCDEF$: $PBQR$ is the displacement loading zone, point B is the point acted by the indenter, PR, QR are cross lines between the top face and the flank face of the indenter, that is, $u_{zP} = u_{zQ} = u_{zR} = 0$, other part of the face is free.

(4) Other faces are free.

4 NUMERICAL CALCULATION METHOD ——MOL AND MAL

The semi-analytic method of lines (MOL) and method of arbitrary of lines (MAL), which are suitable for the regular zone, are used in the numerical calculation. Compared with method of finite element (MFE), the efficiency and precision of the calculation are higher.

Under elastic state, the Navier-Cauchy equation without the volume force is

$$\mu\nabla^2\boldsymbol{u} + (\lambda + \mu)\nabla\nabla\cdot\boldsymbol{u} = 0 \qquad (10)$$

where $\nabla = \frac{\partial}{\partial x_1}e_1 + \frac{\partial}{\partial x_2}e_2 + \frac{\partial}{\partial x_3}e_3$, $\boldsymbol{u} = (u_1, u_2, u_3) = (u, v, w)$. λ, and μ are Lame constants, here

$$(\lambda, \mu, u) = \begin{cases} (\lambda^+, \mu^+, u^+) & x_2 > 0 \\ (\lambda^-, \mu^-, u^-)\text{ic} & x_2 < 0 \end{cases} \qquad (11)$$

If the discrete of Eq. (10) at point P in Fig. 3 is considered, the equidistance difference equations are

$$\begin{aligned} -u''_{i,j} = {} & (a+1)\frac{1}{H^2}(u_{i,j+1} - 2u_{i,j} + u_{i,j-1}) + \\ & \frac{1}{h^2}(u_{i+1,j} - 2u_{i,j} + u_{i-1,j}) + \\ & \frac{a}{2H}(w'_{i,j+1} - w'_{i,j-1}) + \\ & \frac{a}{4Hh}(v_{+1,j+1} - v_{+1,j-1} - v_{-1,j+1} + \\ & v_{-1,j-1}) \end{aligned} \qquad (12)$$

$$\begin{aligned} -v''_{i,j} = {} & \frac{1}{H^2}(v_{i,j+1} - 2v_{i,j} + v_{i,j-1}) + \\ & \frac{a+1}{h^2}(v_{i+1,j} - 2v_{i,j} + v_{i-1,j}) + \\ & \frac{a}{2h}(w'_{i+1,j} - w'_{i-1,j}) + \\ & \frac{a}{4Hh}(u_{i+1,j+1} - u_{i+1,j-1} - \\ & u_{i-1,j+1} + u_{i-1,j-1}) \end{aligned} \qquad (13)$$

$$\begin{aligned} -(a+1)w''_{i,j} = {} & \frac{1}{H^2}(w_{i,j+1} - 2w_{i,j} + \\ & w_{i,j-1}) + \frac{1}{h^2}(w_{i+1,j} - \\ & 2w_{i,j} + w_{i-1,j}) + \end{aligned}$$

$$\frac{a}{2H}(u'_{i,j+1} - u'_{i,j-1}) + \frac{a}{2h}(v'_{i+1,j} - v'_{i-1,j}) \quad (14)$$

Because the description of point M at interface $BEEB'$ in Fig. 4 in x_2-direction is difficult, the common method can not be used. The general equations of the discrete line at the interface between two mediums are developed. It is based on the discrete equation of the single medium and the continuous conditions at the interface.

Displacement continuous conditions.

$$u^+|_M = u^-|_M$$
$$v^+|_M = v^-|_M$$
$$w^+|_M = w^-|_M \quad (15)$$

Stress continuous conditions

$$\sigma_y^+|_M = \sigma_y^-|_M$$
$$\tau_{xy}^+|_M = \tau_{xy}^-|_M$$
$$\tau_{yz}^+|_M = \tau_{yz}^-|_M \quad (16)$$

Therefore, the general formulas of the discrete lines at the interface are

$$-(\mu^+ + \mu^-)u''_{i,j} = \left|\frac{(a^+ + 1)\mu^+}{H^2} + \frac{(a^- + 1)\mu^-}{H^2}\right| \cdot (u_{i,j+1} - 2u_{i,j} + u_{i,j-1}) + \left|\frac{2\mu^+}{h^2}(u_{i+1,j} - u_{i,j}) + \frac{2\mu^-}{h^2}(-u_{i,j} + u_{i-1,j})\right| + \frac{\mu^+ - \mu^-}{Hh}(v_{i,j+1} - v_{i,j-1}) + \frac{a^+\mu^+ + a^-\mu^-}{2H}(w'_{i,j+1} - w'_{i,j-1}) + \frac{a^+\mu^+}{2Hh}(v_{i+1,j+1} - v_{i+1,j-1} - v_{i,j+1} + v_{i,j-1}) + \frac{a^-\mu^-}{2Hh}(v_{i,j+1} - v_{i-1,j+1} - v_{i,j-1} + v_{i-1,j-1}) \quad (17)$$

$$-(\alpha^+ + \alpha^-)v''_{i,j} = \frac{1}{H^2}(\alpha^+ + \alpha^-)(v_{i,j+1} - 2v_{i,j} + v_{i,j-1}) + \frac{4\mu^+(1+d^+)}{h^2}(v_{i+1,j} - v_{i,j}) + \frac{4\mu^-(1+d^-)}{h^2}(-v_{i,j} + v_{i-1,j})] + (\frac{4\mu^+ d^+}{h} - \frac{4\mu^- d^-}{h})(w'_{i,j} + \frac{u_{i,j+1} - u_{i,j-1}}{2H}) + [\frac{a^+ a^+}{h}(w'_{i+1,j} - w'_{i,j}) + \frac{a^- a^-}{h}(w'_{i,j} - w'_{i-1,j})] + [\frac{a^+ a^+}{2Hh}(u_{i+1,j+1} - u_{i,j+1} - u_{i+1,j-1} + u_{i,j-1}) + \frac{a^- a^-}{2Hh}(u_{i,j+1} - u_{i-1,j+1} - u_{i,j-1} + u_{i-1,j-1})] \quad (18)$$

$$-[\mu^+(1+a^+) + \mu^-(1+a^-)]w''_{i,j} = \frac{\mu^+ + \mu^-}{H^2}(w_{i,j+1} - 2w_{i,j} + w_{i,j-1}) + [\frac{2\mu^+}{h^2}(w_{i+1,j} - w_{i,j}) + \frac{2\mu^-}{h^2}(-w_{i,j} + w_{i-1,j})] + \frac{2(\mu^+ - \mu^-)}{h^2}v'_{i,j} + \frac{a^+ a^-}{2H}(\mu'_{i,j+1} - \mu'_{i,j-1}) + [\frac{a^+}{h}(v'_{i+1,j} - v_{i,j}) + \frac{a^-}{h}(v'_{i,j} - v'_{i-1,j})] \quad (19)$$

where subscript (i, j) represents line i, row j discrete line, $a = \frac{1}{1-2v}$, $d = \frac{v}{1-2v}$, $a = \frac{\mu(1+\alpha)(1-2v)}{1+a}$, H and h are the difference distances in the directions x_1 and x_2 respectively. Eq. (17) ~ (19) are the difference equation in the direction x_1, x_2, x_3 respectively. It is obvious that Eqs. (17) ~ (19) are the same as Eqs. (12) ~ (14) when the two mediums at two sides of the interface are alike.

It should be point out that (1) Eqs. (17) ~ (19) yet need to be improved for left, right edge lines corresponding to point B, E at the interface in Fig. 3 by the method similar to single medium, (2) the free changing-distance difference is used in the numerical calculation because the equidistance difference is inconvenient.

For convenience, the changing-distance difference equation of the second-order derivate of an arbitray function $f(x)$ is given only

$$f''_i = \frac{h_{i-1}f_{i+1} - (h_{i-1} + h_i)f_i + hf_{i-1}}{h_{i-1}h_i(h_{i-1} + h_i)/2} \quad (20)$$

where $h_i = x_{i+1} - x_i$, f_i is the functional value $f(x_i)$ at discrete point i. After the displacement vector of nodal line is introduced, we have

$$\underline{u}^* = [u_1, v_1, w_1, u_2, v_2, w_2, \cdots, u_n, v_n, w_n]^T \quad (21)$$

Considering boundary condition, we have

$$\text{or} \quad \begin{matrix} \sigma_{i,j} n_i = \overline{X} \\ u_i = \overline{u}_i \end{matrix} \quad (22)$$

The ordinary differential equation group can be obtained

$$\underline{u}^{*''} = \underline{A}\underline{u}^{*'} + \underline{B}\underline{u}^* + \underline{F} \quad (23)$$

substituing Eq. (21) into Eq. (22), the discrete boundary conditions can be obtained. Considered the conditions, $\underline{F}$ occurs in Eq. (23).

MAL results from the combination of MOL with MFE. At first, the units are divided and changed into regular units if necessary, and then the displacement field in a unit is described approximatively by the interpolation of the nodal line that is an unknown quantity. The second, on the basis of the conservation of energy, the ordinary differential equation group, which is similar to Eq. (23), is obtained.

5 UNIT DIVIDING

Although the size of the loading zone is much smaller than that of dcalculated model, one unit is divided at least in the zone. On the other hand, because of the limitation of computer contain, it is impossible that the size of others is not as same as that of the unit in the zone, that is, the farther from loading zone, the larger the size of unit. It is ensured that the interface between the units is at the interface between the coating and the substrate.

The difference in unit dividing between MAL and MFE is that in MAL the nodal line is retained in a direction (direction z) and the units are the three dimension units which are surrounded by nodal line and end surface, the displacements of the nodal line in the direction x, y, z and their first-order derivate in the direction coordinate of the line are the quantities to be solved, they are solved by the ordinary differential equation, and then each physical quantity is solved. The unit dividing is shown in Fig. 4.

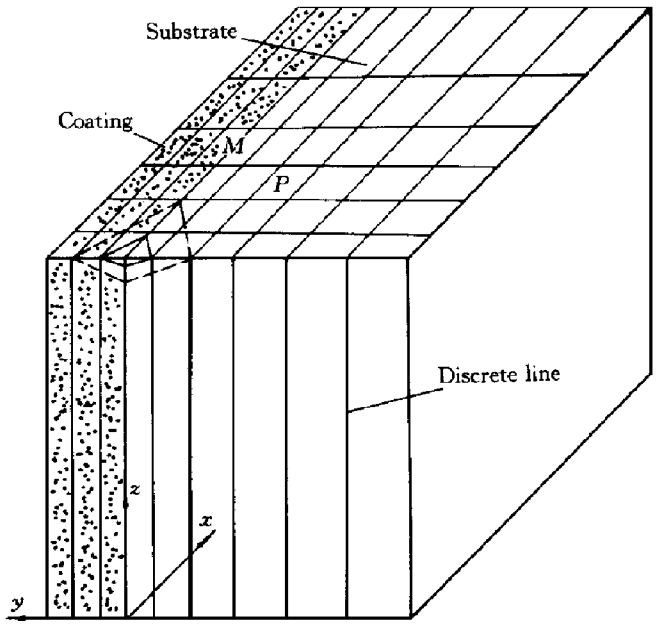

Fig. 4 Discrete line and change of indentation depth

6 CALCULATION EXAMPLE

6.1 Calculation of load vs depth curve at elastic state without crack

At first, the normal stress (σ_z) of the loading zone in direction z, which corresponds to the indentation depth from zero to h_{max} (the depth of point C in Fig. 2), is calculated, and the load value (F_i) is solved from mean value of σ_z in each nodal point and unit area. Load (F) ~ indentation depth (h) curve is obtained by n times iteration. The specimen of 0.6 mm thick Al_2O_3 coating/40Cr steel substrate is taken as an example. The elastic modulus of 40Cr steel is 202 GPa[7], Al_2O_3 coating 360 MPa[8]. The calculated result of the specimen is listed in Tab. 1. When the indentation depth on the specimen is 0.032 mm, the calculated value of load is 151.27 N, and experimental value F_w is 102.5 N. Although the relative deviation between the two value is 30%, this indicates that the mechanical analysis and numerical calculation are feasible.

6.2 Calculation of opening displacement field of interface

In order to calculate the opening displacement field of the interface, the discrete line is parallel to y axis. The opening displacement field of the surface, which is parallel to xoy plane, is calculated by the plane stress method, the field of the interface on symmetric plane yoz is calculated by the plane strain method, and the field of other part is calculated by smooth transition. The schematic is shown in Fig. 5. After the displacement field is calculated, the approximate bonding stress value is obtained from Eq. (8). For example, the calculated value of the opening displacement field of Al_2O_3 coating/40Cr substrate specimen is shown in Fig. 6. From the result of the displacement field, the calculated value of the load (F_c= 151.27 N) and the experimental result of the load (F_w= 102.5 N), the calculated value of the bonding stress is equal to 31.49 MPa. The relative deviation between the value and the result measured by pull-off method (σ_{ad}= 21 MPa) is about 30%. Therefore, the load ~ indentation depth curve and critical load F_w are measured by the new indentation tester, and the bonding stress is obtained by numerical calculation.

Table 1 Calculation result of loading curve of Al_2O_3/40Cr

Indentation depth/mm	Load/N
0.0114	6.58
0.0171	23.56
0.0229	56.73
0.0317	151.27

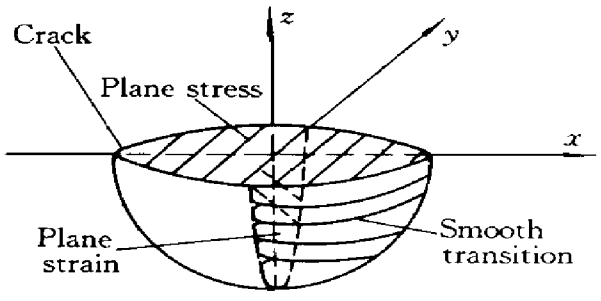

Fig. 5 Schematic of numerical calculation of crack opening displacement field

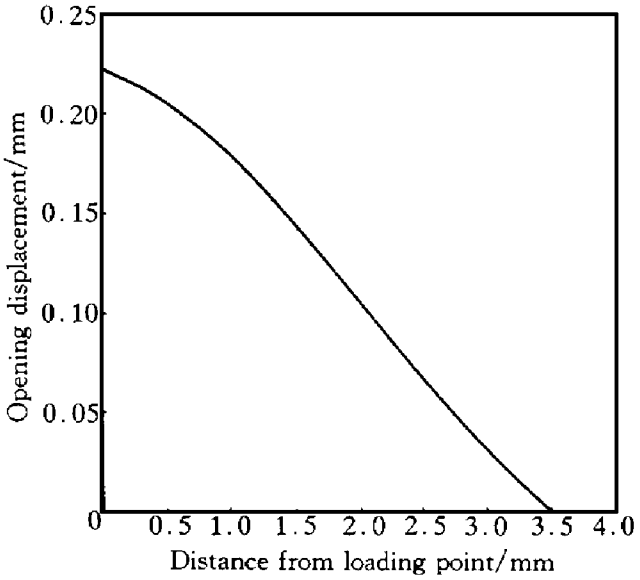

Fig. 6 Opening displacement on bank of interface crack in Al_2O_3/40Cr

REFERENCES

1 Zheng Senlin and He Jiawen. Science and Technology of Thin Films, (in Chinese), 1993, 6(2): 85- 90.
2 Rhyim Y M and Park C G. In: Proceedings of 14th ITSC. Japan: 1995: 773- 778.
3 Lesage J. In: Proceedings of 14th ITSC. Japan, 1995: 891- 896.
4 Yi Maozhong, Hu Naisai and He Jiawen. CN ZL94243811.6.
5 Yi Maozhong, Ran Liping, Dai Yao and He Jiawen. Physical Testing and Chemical Analysis, Part A: Physical Testing, (in Chinese), 1998, (1): 27- 30.
6 Dai Yao, He Jiawen and Yi Maozhong. In: Proceedings 14th ITSC, Japan, 1995: 957- 959.
7 Sun Zhenbao. Handbook of Alloy Steels, (in Chinese). Beijing: Metallurgical Industry Press, 1992: 260.
8 Kawase R. In: Proceedings of 3th National Thermal Spray Conf. USA, 1990: 339- 342.

(Edited by Zhu Zhongguo)